Proposal of a One-DOF Actively Controlled Bearingless Motor Using Zero-Sequence Current

Yusuke FUJII [a]

a Tokyo Institute of Technology, 2-12-1 Ookayama, Meguro, Tokyo, Japan, fujii@ee.e.titech.ac.jp

Abstract

This paper proposes a one-DOF actively controlled bearingless motor with 1 kW output power using a three-phase four-wire inverter system equivalent to a three-phase inverter in terms of the number of power-switching devices. In the proposed system, the thrust suspension winding is connected between the neutral point of the Y-connected motor windings and the middle point of the two capacitors in the DC link. The zero-sequence current flowing into the thrust suspension winding generates active thrust force, while the motor is driven by dq-axis vector control. The flux of bias PMs for the thrust magnetic suspension is not flowing into the motor stator core, and the proposed motor design is superior to the conventional design. Additionally, the flux, which is generated by the zero-sequence current flowing into the motor winding, contributes to increasing the thrust force. To demonstrate the performance of both the motor and magnetic suspension, FEA was conducted. It was found that the proposed bearingless motor system has a potential to achieve both stable magnetic suspension and 1 kW-output.

Keywords: *Bearingless motor, Magnetic bearing, Magnetic suspension, Permanent magnet motor, Zero-sequence current*

1. Introduction

Bearingless motors generate rotational torque while the rotor is suspended in a non-contact manner, therefore overcoming many problems related to mechanical bearings. To achieve magnetic suspension in non-contact manner, three translational (x, y, z) and two tilting (θx, θy) motions of the rotor must be magnetically stabilized. Although five-degree-of-freedom (DOF) controlled bearingless motors which actively regulate all of the rotor motions have been developed (Asama, et al., 2010) and (Baumgartner, et al., 2014), they require numerous permanent magnets (PMs), electromagnets, and inverters. Therefore, five-DOF bearingless systems have higher cost and larger size.

A reasonable solution for simplification of the bearingless system is to minimize the number of active magnetic suspensions. One-DOF actively controlled bearingless motor has been developed (Bauer, et al., 2014).The axial force was generated by regulating a suspension current superimposed onto three-phase motor currents. Although the machine is effective for downsizing and simplification of the system, the system requires six half-bridges for independently regulating three types of currents. Another one-DOF actively controlled bearingless system utilizing a single-phase motor has been developed (Gruber, et al., 2019). The axial force was generated by regulating a suspension current superimposed onto single-phase motor currents. The system requires four half-bridges for independently regulating two types of currents. General vector control with dq-axis currents cannot be performed because of the single-phase motor. For further system simplification, single-drive bearingless motors with one-axis active positioning have been developed: axial-gap type (Asama, et al., 2021) and radial-gap type (Sugimoto, et al., 2017). The axial force and torque are generated by d- and q-axis currents, respectively. The remaining radial and tilting positions (x, y, θx, and θy) are passively stabilized by repulsive passive magnetic bearings (RPMB) consisting of the stator PMs and rotor PMs. The system is driven by only one three-phase voltage source inverter. However, flux weakening control with dq-axis vector control, which is able to extend the rotational region with high efficiency, cannot be applied to the single-drive bearingless motor because the d-axis current is dedicated to the axial positioning. Moreover, as far as the authors know, one-DOF controlled bearingless motor over 1 kW has never been reported.

This paper proposes a one-DOF actively controlled bearingless motor with 1 kW using a three-phase four-wire inverter system equivalent to three-phase inverter in terms of the number of power switching devices. In the proposed system, the thrust suspension winding is connected between the neutral-point of the Y-connected motor windings and the middle point of the two capacitors in the DC link. The zero-sequence current flowing into the thrust suspension winding generates active thrust force, while the motor is driven by dq-axis vector control. This paper describes a proposed system including bearingless structure, power electronics circuit, and suspension principle, and then FEA results show the performance of the proposed bearingless motor.

2. Proposed system

2.1 Three-phase four-wire inverter using zero-sequence current

Fig. 1 shows a proposed circuit using a zero-sequence current, i_z (Fujii, et al., 2021). The DC link is divided by two capacitors. The thrust suspension winding is connected between the neutral-point of the Y-connected motor windings and the middle point of the two capacitors. The current flowing into this line is defined as the zero-sequence current i_z, and consequently it generates active thrust suspension force while the three-phase motor is driven with dq-axis vector control, without additional power switching device.

When motor drive and magnetic suspension are performed, the phase currents (i_u, i_v, and i_w) and the terminal voltages (v_u, v_v, and v_w) are expressed as follows:

$$\begin{aligned} i_u(t) &= I_m \cos(\omega_m t + \beta) + i_z(t)/3 \\ i_v(t) &= I_m \cos(\omega_m t + \beta - 2\pi/3) + i_z(t)/3 \\ i_w(t) &= I_m \cos(\omega_m t + \beta - 4\pi/3) + i_z(t)/3 \end{aligned} \quad (1)$$

$$\begin{aligned} v_u(t) &= V_m \cos(\omega_m t + \phi) + v_z(t) \\ v_v(t) &= V_m \cos(\omega_m t + \phi - 2\pi/3) + v_z(t) \\ v_w(t) &= V_m \cos(\omega_m t + \phi - 4\pi/3) + v_z(t) \end{aligned} \quad (2)$$

where V_m represents the amplitude of the motor voltage, v_z represents the zero-sequence voltage, ω_m represents the angular frequency of the motor, and ϕ represents the initial phase. As shown in (2), the zero-sequence voltage v_z in phase is superimposed onto each terminal voltage. Substituting $V_m = 0$ into (2) yields,

$$v_u(t) = v_v(t) = v_w(t) = v_z(t) \quad (3)$$

Fig. 2 shows a zero-sequence equivalent circuit based on (3). The three-phase four-wire inverter system offers a half-bridge function in addition to the three-phase voltage inverter. It should be noted that the zero-sequence current must not have a DC component because the zero-sequence DC current unbalances the two capacitors. Therefore, the zero-power control is required in thrust magnetic suspension so that the zero-sequence DC current is eliminated.

2.2 Structure

Fig. 3 shows the structure of the proposed one-DOF actively controlled bearingless motor, which consists of the repulsive passive magnetic bearing (RPMB), thrust magnetic suspension, and motor units. The RPMBs are placed at the top and bottom ends of the machine, the radial and tilting positions (x, y, θx, and θy) are passively stabilized by the RPMBs. The inner and outer diameters of the rotor repulsive PMs are 37 mm and 53 mm, respectively, with a height of 7.5 mm. The inner and outer diameters of the stator repulsive PMs are 59 mm and 74 mm, respectively, with a height of 7.5 mm. The thrust magnetic suspension unit is configured with the yoke, thrust core, thrust suspension windings with ring shape, and upper/lower bias PMs. The motor unit placed in the center is configured with laminated stator core that has 12-slots, three-phase 8-pole motor concentrated windings, rotor core and motor PMs. The inner and outer diameters of the stator are 60 mm and 110 mm, respectively. The outer diameter of the upper/lower bias PMs and motor PMs in the rotor is 53 mm. The air gaps in the radial direction of the RPMBs and the motor units are set to 3.0 mm and 3.5 mm, respectively, as comparatively wide gap is needed to avoid the touch-down of rotor in the radial direction. The grades of the repulsive PMs and rotor PMs (upper/lower bias and motor) are N52 and N48, respectively.

Fig. 4 shows the magnetization direction of the rotor PMs. Each upper and lower bias PM is magnetized in a unipolar direction and generates a bias flux for the thrust magnetic suspension. Additionally, the flux of bias PMs is not flowing into the motor stator core, thus it has no significant influence on the motor performance.

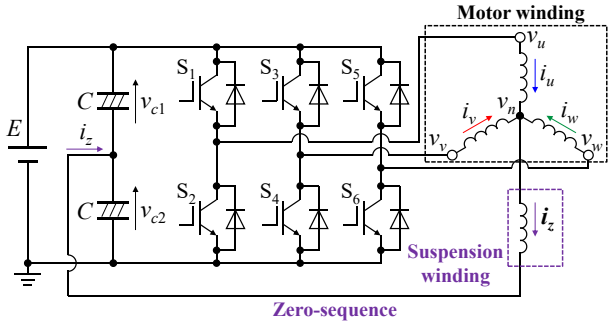

Figure 1 Proposed circuit using zero-sequence current, i_z.

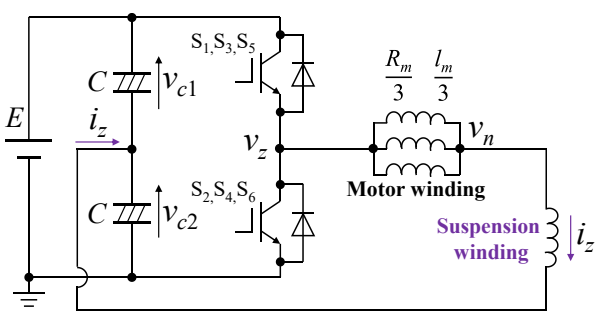

Figure 2 Zero-sequence equivalent circuit.

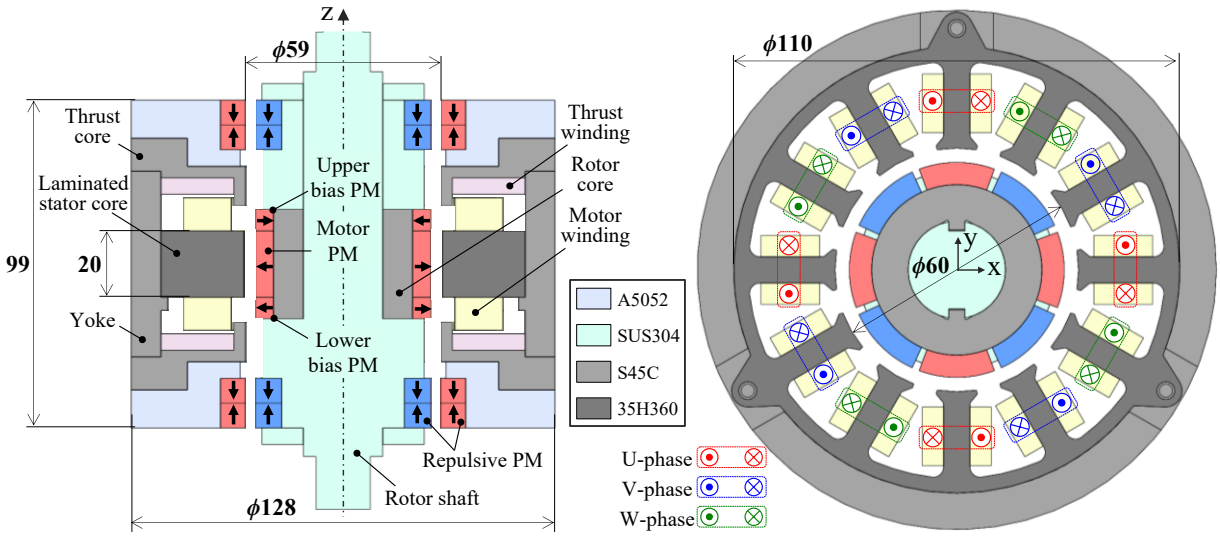

Figure 3 Structure of the Proposed bearingless motor: cross-sectional view of entire model (left) and motor unit (right), respectively.

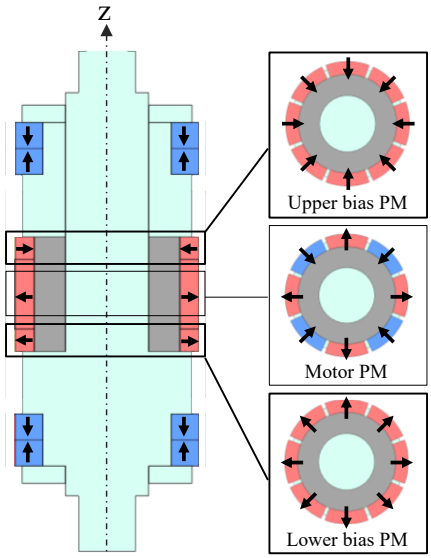

Figure 4 Magnetization direction of rotor PMs.

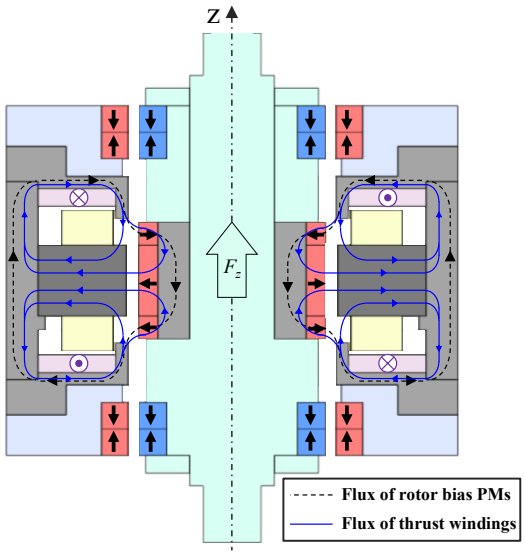

Figure 5 Principle of thrust magnetic suspension.

2.3 Principle of magnetic suspension

Fig. 5 shows the principle of the thrust magnetic suspension, where the positive zero-sequence current is provided into the thrust suspension windings. As indicated by the dotted line in Fig. 5, the flux of the bias PMs passes and loops through the upper bias PMs, rotor core, lower bias PMs, thrust core, and yoke. As indicated by the solid line in Fig. 5, the suspension flux, which is generated by providing the thrust suspension winding with zero-sequence current, passes and loops through the thrust core, rotor core, stator core, and yoke. The flux in the axial direction between the thrust core and rotor core in the upper side becomes denser than that in the lower side, and consequently positive thrust force, F_z, is generated in the rotor. Likewise, the negative thrust force is generated by the negative zero-sequence current.

As indicated in (1), the zero-sequence current for the thrust magnetic suspension flows in the motor windings in addition to the thrust suspension windings. The zero-sequence current $i_z(t)/3$ flowing in the motor windings is denoted as “motor zero-sequence current” herein in order to distinguish it from the zero-sequence current flowing in the thrust suspension windings. The flux generated by the motor zero-sequence current passes and loops through the same place as the thrust suspension flux of Fig. 5. Therefore, it is worth noting that the motor zero-sequence current contributes to increasing the thrust force.

3. FEA analysis

To demonstrate the performance of the proposed one-DOF controlled bearingless motor, three-dimensional (3D) finite element analysis (FEA) was performed using the model shown in the second section.

3.1 Motor torque

Fig. 6 shows the relationship between the torque T and the motor current density J_m. The torque reached 2.87 Nm at a motor current density of 8 A_{rms}/mm^2 (equal to a phase current of 20.1 A_{rms}), which is the rated current. Therefore, the motor is able to achieve 1 kW under the rated current at 3328 rpm.

Fig. 7 shows the torque waveforms at a motor current density of J_m = 8 A_{rms}/mm^2 when providing zero-sequence current. J_z represents the current density of the thrust suspension winding. The torque waveform at J_z = 0 A/mm^2 was identical with that at J_z = 4 A/mm^2. This result implies that the zero-sequence current has no influence on the torque.

3.2 Passive suspension

Fig. 8 shows the force in the x-axis, F_x, acting on the rotor when the rotor is displaced in the x-axis direction, where the average of F_x in one cycle of electrical rotation is plotted. The restoring force was generated by the RPMBs and the rotor positions in the passive directions are stabilized. The total stiffness in the x-axis direction reached 60 N/mm at an x-position of 1.0 mm.

Fig. 9 shows the unbalanced magnetic pull force (UMF) acting on the rotor when the rotor is displaced in the z-axis direction, where the average of the UMF in one cycle of electrical rotation is plotted. The UMF in the z-axis direction was caused by the RPMBs, and was equal to 128 N at the z-position of 0.4 mm in the start-up of the magnetic suspension. Hence, to achieve the thrust magnetic suspension, the active thrust force needs at least 128 N.

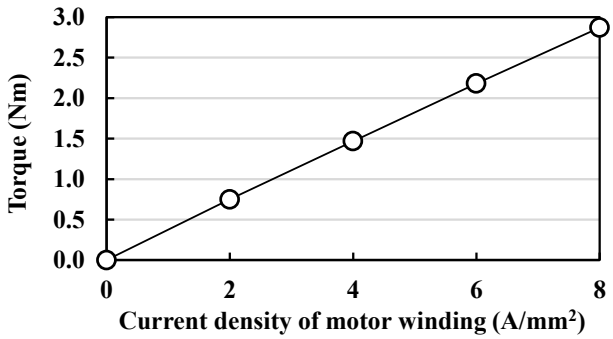

Figure 6 Relationship between torque and motor current density.

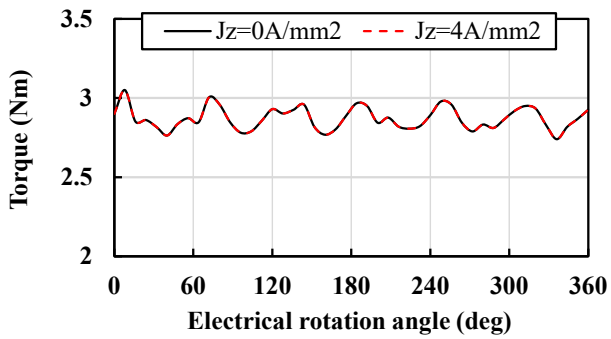

Figure 7 Torque when providing zero-sequence current.

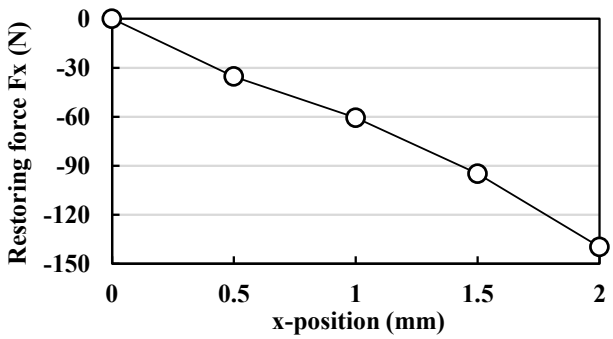

Figure 8 Restoring force in the x-axis direction.

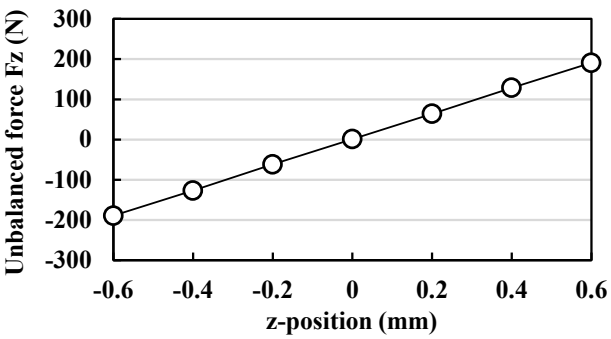

Figure 9 Unbalanced magnetic pull force in the z-axis direction.

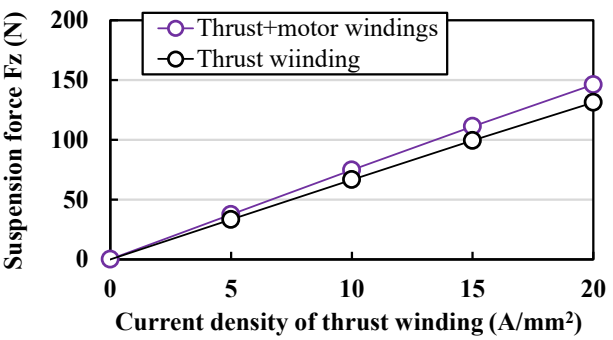

Figure 10 Relationship between thrust force and zero-sequence current.

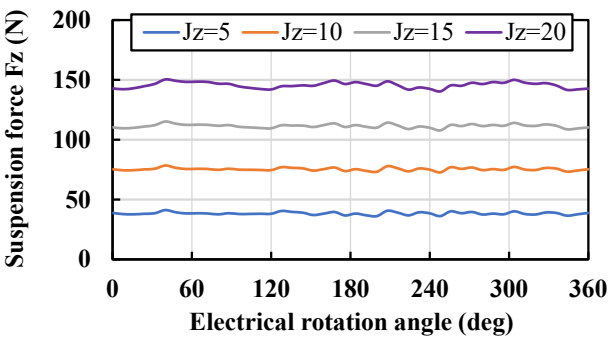

Figure 11 Thrust force waveforms.

3.3 Active thrust magnetic suspension

Fig. 10 shows the relationship between the active thrust suspension force F_z and the thrust current density J_z. The thrust force was increased by the zero-sequence current flowing into not only the thrust suspension winding, but also into the motor winding, and reached 146 N at J_z = 20 A/mm^2, which exceeds the UMF in the z-axis direction at the start-up.

Fig. 11 shows the waveforms of the thrust suspension force, Fz. The ripple of the thrust force depending on the rotational angle was comparatively small.

4. Conclusion

This paper proposed a one-DOF actively controlled bearingless motor with 1 kW output power, using a three-phase four-wire inverter system. In the proposed system, the thrust suspension winding is connected between the neutral-point of the Y-connected motor windings and the middle point of the two capacitors in the DC link. The zero-sequence current flowing into the thrust suspension winding generates active thrust force, while the motor is driven by dq-axis vector control. The flux of bias PMs for the thrust magnetic suspension is not flowing into the motor stator core, and the proposed motor design is superior to the conventional design. The 3D-FEA results demonstrated that the proposed motor has a potential to achieve both stable magnetic suspension in a non-contact manner and a 1 kW-output.

References

Asama J, Amada M, Tanabe N, Miyamoto N, Chiba A, Iwasaki S, and Takemoto M (2010) Evaluation of bearingless PM motor with wide magnetic gaps. IEEE Trans. Energy Convers., vol. 25, no. 4, pp. 957–964.

Asama J, Tai T, and Chiba A (2021) Development of axial-flux single-drive bearingless motor with one-axis active positoning. IEEE Trans. Ind. Appl., vol. 57, no. 6, pp. 6792–6799.

Baumgartner T, Burkart R, and Kolar J (2014) Analysis and design of a 300-W 500 000-r/min slotless self-bearing permanent-magnet motor. IEEE Tran. Ind. Electron, vol. 61, no. 8, pp. 4326–4336.

Baur W, Freudenthaler P, and Amrhein W (2014) Experimental characterization of a bearingless rotating field axial-force/torque motor. In: 14th International Symposium Magnetic Bearings, 2014, pp. 132–137.

Fujii Y, Asama J, and Chiba A (2021) Voltage sensorless control of split capacitor for three-phase four-wire motor system with zero-sequence suspension winding. IEEE Trans. Ind. Appl., vol. 57, no. 6, pp. 6823-6832.

Gruber W, Baur W, Wetsch D, Klammer B, and Kurita N (2019) Implementation of a bearingless axial-force/torque motor fan with flex-PCB windings. In: 2019 International Electric Machines and Drives Conference, 2019, pp. 179–184.

Sugimoto H, Shimura I, and Chiba A (2017) A novel stator structure for active axial force improvement in a one-axis actively positioned single-drive be aringless motor. IEEE Trans. Ind. Appl., vol. 53, no. 5, pp. 4414-4421.